16th World Conference on Earthquake Engineering, 16WCEE 2017
Santiago Chile, January 9th to 13th 2017
Paper N° 874 (Abstract ID)
Registration Code: S-R1460549049

RELATIVE IMPORTANCE OF HORIZONTAL AND VERTICAL COMPONENTS OF EARTHQUAKE MOTION ON THE RESPONSES OF BARREL VAULT CYLINDRICAL ROOF SHELLS

S. Ostovari Dailamani (1), J. G.A. Croll(2)

(1) *Emeritus Professor of Civil Engineering, University College London (UCL), j.croll@ucl.ac.uk*
(2) *Senior Lecturer, University of Greenwich, os36@gre.ac.uk*

Abstract

During earthquake events, Civil Engineering structures are subjected to three components of earthquake. While these structures have been extensively investigated for horizontal component of earthquakes, there have been relatively few studies on the vertical ground motion. The few published studies of the effects of the vertical components of earthquakes on reinforced concrete bridges indicate that some failures during large earthquakes have been due to the vertical ground motions.

There are also indications that thin shells are once again becoming a popular option for roofs covering large column free spaces. Especially in the seismically active regions, it is important to incorporate into design, consideration of how they will respond to the effects of vertical component of earthquake loading. However, the few past studies of the performance of roof shells in earthquake have been largely performed for the horizontal components of earthquake with the vertical component neglected.

In this paper a semi-analytical method, which has been previously verified using a finite element modelling, is used to find the forced vibration response when barrel vault cylindrical shells are subjected to synchronous vertical motions recorded from typical earthquake records. The analytical method adopts an explicit solution based upon the Love-Timoshenko strain-displacement relationships and employs a Lagrangian approach to the derivation of the equations of motion.

The assessment of the relative importance of the horizontal and vertical components of earthquakes shows that vertical components result in higher accelerations and stresses compared to the horizontal components.

Keywords: Barrel vault cylindrical roof shells; vertical components of earthquakes; design of roof shells

1. Introduction

The prevalence of very efficient and robust shell structures in nature has been a source of inspiration for many engineers.

During the event of earthquake civil engineering structures are subjected to three components of earthquake. Civil engineering structures have been extensively investigated for horizontal component of earthquakes. However, there have been relatively few studies on the vertical ground motion. A few published research on the effect of the vertical component of earthquake on Reinforced Concrete (RC) bridges indicate that some failure have been observed during large earthquakes due to the vertical ground motion [1] [2]. The field observation of the past earthquakes during the past 20 years such as in Northridge (1994) and Hyogo-ken Nanbu (1995) also reports sever damages to structures as a result of vertical component of the earthquakes [2].

For the first time in 2008, the result of a study investigating the effect of vertical component of ground motion on two-span highway bridges revealed that the Seismic Design Criteria (SDC) used by the California Department of Transportation needs to take into account the effect of vertical component of earthquakes [3]. It is worthy to mention that for the peak ground acceleration higher than 0.6 g, SDC demands the vertical component of ground motion to be considered as a uniformly distributed vertical load equal to 25% of the dead load. However, it is not required to analyse the structure under the combined horizontal and vertical components of the earthquake.

Recent research also shows that the near field earthquakes may have a higher ratio of vertical to horizontal Peak Ground Acceleration (PGA) than the far field earthquakes. The result of one investigation also shows that the ratios of vertical to horizontal spectral acceleration are higher for higher frequencies than for the lower frequencies [4]. Therefore, neglecting the vertical component of ground motion underestimates the responses of structures with high frequency content such as roof shells.

After examining the response spectra of the vertical motion of Northridge earthquake, Bozorgnia et al found that the ratio of the vertical to horizontal response spectra are highly dependent on the period and site distance to source [5]. Their study among many other studies [6][7][8][9] also shows that the code recommendation based on the vertical component of the earthquake being 2/3 of the horizontal value underestimates the effect of the vertical component of the earthquake as they can be higher than 2/3 of the horizontal values. Among these studies, a study by Kim et al who selected a subset of 452 relatively large earthquake records [10] and with the PGA of 0.1 g or more from the Pacific Earthquake Engineering Research next generation attenuation project database can be named [10]. Their study shows that limiting the ratio of V/H to 2/3 seriously underestimates the effect of vertical component of earthquake on structures for the case of near-field earthquakes and overestimates the earthquakes at far-field events.

Moreover, scaling the horizontal component of earthquake to obtain the vertical earthquakes, as suggested by many design codes, does not give realistic indication of the vertical component of earthquake. It is due to the different energy content of vertical and horizontal components of the earthquake. As it will be shown in the present research and also shown by previous researchers [10], the energy content of vertical earthquakes is concentrated in a narrow high frequency band. This can significantly affect the response of structures in short period range; such as the period of reinforced concrete structures especially roof shells.

As shown by Elnashai and Papazoglou [9] the high frequency content of the vertical ground motion results in significant response amplification. They have shown that the changes in forces are more significant than displacements. The results from the present study also confirm significant amplification in the forces and accelerations in comparison with the displacements.

The present investigation shows that as the forces and moments are corresponding to the first and second derivatives of displacements, in roof shells the modes corresponding to the high frequencies contribute significantly to the response. Therefore, the modes with larger half waves in axial and circumferential directions have significant contribution to the changes in forces, accelerations, and bending moments for roof shells when subjected to vertical ground motion.

As explained, the literature suggests that more investigation is needed on the effect of the vertical ground motion on structures. Among different civil engineering structures shell structures are one of the most efficient ones. As a result, shell structures have also been exploited in different areas of science and technology.

Roof shells are one kind of shell structures, which are used for covering large column free spaces. Despite the numerous past research dealing with the free vibration of shells [11][12], it was noticed that very little has been published on the earthquake response of roof shells. If roof shells are designed properly, they can also serve as shelter for people who have lost their homes during the earthquake. So it is surprising to see the little studies on the earthquake responses of roof shells.

Yamada [13] has studied latticed cylindrical roofs using an equivalent isotropic cylindrical shell, and Kunieda [14] reports an investigation of elastic responses of spherical domes and cylindrical roof shells subjected to either horizontal or vertical components of earthquakes.

The little studies suggest that there is a need for investigating the relative importance of vertical and horizontal ground motion for roof shell. Moreover, from the above-mentioned limited studies it is difficult to draw general conclusions, indicating a need for rather more systematic investigations of the earthquake response of shells. However, any new contribution to the existing literature needs to be cross-checked to ensure its validity and numerical accuracy. In a previous paper authors developed an analytical method to find the response of roof shells to earthquake. The analytical method that will be described in this paper has been cross-checked with the available literature and FE programmes.

The analytical approach described in the following is used in this paper to assess the relative importance of vertical and horizontal components of earthquake motion in the displacement, acceleration, and stress responses of the roof shell.

2. Analytical modelling

An analytical model is developed for a thin, open cylindrical shell, of radius of curvature R, longitudinal length $L_x = L$, thickness h, and opening angle ϕ as shown in Fig.1.

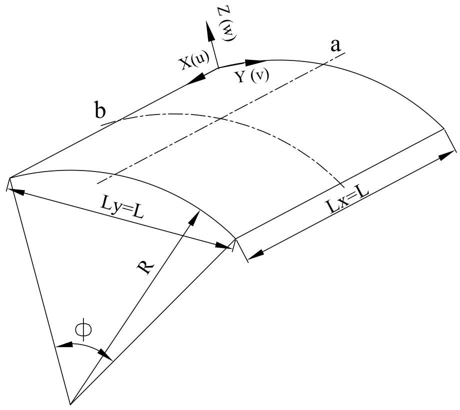

Fig. 1 – Geometry of shell

Material is taken to be linearly elastic, and the damping ratio is taken to be constant in all modes. The strain-displacement relationships are derived using the equations of Love and Timoshenko [1]. The strains at a distance z from the middle surface may be represented as

$$\epsilon_x = \epsilon'_x - z\chi_x; \quad \epsilon_y = \epsilon'_y - z\chi_y; \quad \epsilon_{xy} = \epsilon'_{xy} - 2z\chi_{xy} \tag{1}$$

where the membrane and bending strains of the mid-surface are

$$\begin{aligned} \epsilon'_x &= \frac{\partial u}{\partial x}, \qquad \chi_x = -\frac{\partial^2 w}{\partial x^2} \\ \epsilon'_y &= \frac{\partial v}{\partial y} + \frac{w}{R}, \quad \chi_y = -\frac{\partial^2 w}{\partial y^2} + \frac{1}{R}\frac{\partial v}{\partial y} \\ \epsilon'_{xy} &= \frac{\partial u}{\partial y} + \frac{\partial v}{\partial x}, \quad \chi_{xy} = -\frac{\partial^2 w}{\partial x \partial y} + \frac{1}{R}\frac{\partial v}{\partial x} \end{aligned} \tag{2}$$

in which u, v are the axial and circumferential (in-plane) displacement, and w is the lateral (out-of-plane) displacement. Based upon linear elastic, plane stress relationships [11], the membrane and bending stress resultants may be derived as

$$\begin{aligned} N_x &= K(\frac{\partial u}{\partial x} + \nu\frac{\partial v}{\partial y} + \nu\frac{w}{R}) \qquad M_x = D(-\frac{\partial^2 w}{\partial x^2} - \nu\frac{\partial^2 w}{\partial y^2} + \frac{\nu}{R}\frac{\partial v}{\partial y}) \\ N_y &= K(\frac{\partial v}{\partial y} + \frac{w}{R} + \nu\frac{\partial u}{\partial x}) \qquad M_y = D(-\nu\frac{\partial^2 w}{\partial x^2} - \frac{\partial^2 w}{\partial y^2} + \frac{1}{R}\frac{\partial v}{\partial y}) \\ N_{xy} &= K\frac{1-\nu}{2}(\frac{\partial u}{\partial y} + \frac{\partial v}{\partial x}) \qquad M_{xy} = -D(1-\nu)(-\frac{\partial^2 w}{\partial x \partial y} + \frac{1}{R}\frac{\partial v}{\partial x}) \end{aligned} \tag{3}$$

where extensional stiffness $K = \frac{Eh}{1-\nu^2}$, flexural stiffness $D = \frac{Eh^3}{12(1-\nu^2)}$, E=modulus of elasticity, and ν =Poisson's ratio.

2.1 Natural Frequency Extraction

The equations of motion for a shell undergoing a free vibratory motion, where the damping is neglected, are derived by Euler-Lagrange equations

$$-\frac{\partial}{\partial x}\frac{\partial L}{\partial u_x}-\frac{\partial}{\partial y}\frac{\partial L}{\partial u_y}-\frac{\partial}{\partial t}\frac{\partial L}{\partial \dot{u}}=0$$
$$-\frac{\partial}{\partial x}\frac{\partial L}{\partial v_x}-\frac{\partial}{\partial y}\frac{\partial L}{\partial v_y}-\frac{\partial}{\partial t}\frac{\partial L}{\partial \dot{v}}=0$$
$$\frac{\partial L}{\partial w}+\frac{\partial^2}{\partial x^2}\frac{\partial L}{\partial w_{xx}}+\frac{\partial^2}{\partial y^2}\frac{\partial L}{\partial w_{yy}}+\frac{\partial^2}{\partial x\partial y}\frac{\partial L}{\partial w_{xy}}-\frac{\partial}{\partial t}\frac{\partial L}{\partial \dot{w}}=0 \qquad (4)$$

where, $()_x=\frac{\partial}{\partial x}$, and $()_y=\frac{\partial}{\partial y}$, the Lagrangian $L=T-U$, in which the strain energy U, considered in its constituent parts is

$$U=\frac{1}{2}\int_{-\frac{h}{2}}^{+\frac{h}{2}}\int_0^L\int_0^{R\phi}[\sigma_x\epsilon_x+\sigma_y\epsilon_y+\sigma_{xy}\epsilon_{xy}]dxdydz \qquad (5)$$

and the kinetic energy, T, is defined as

$$T=\frac{1}{2}\rho h\int_0^L\int_0^{R\phi}[(\frac{\partial u}{\partial t})^2+(\frac{\partial v}{\partial t})^2+(\frac{\partial w}{\partial t})^2]dxdy \qquad (6)$$

Making use of the Eq. (5),(6) and employing the strain-displacement relations (Eq. (2)), the Euler-Lagrange equations of Eq. (4) will be simplified to the differential equations of motion;

$$S_x(u,v,w)+\rho\times h\frac{\partial^2 u}{\partial t^2}=0$$
$$S_y(u,v,w)+\rho\times h\frac{\partial^2 v}{\partial t^2}=0 \qquad (7)$$
$$S_z(u,v,w)+\rho\times h\frac{\partial^2 w}{\partial t^2}=0$$

Where $S_x(u,v,w)$, $S_y(u,v,w)$, and $S_z(u,v,w)$ are static equation of equilibrium for cylindrical shell in the form of

$$S_x(u,v,w)=-K(\frac{\partial^2 u}{\partial x^2}+\frac{1+\nu}{2}\frac{\partial^2 v}{\partial x\partial y}+\frac{1-\nu}{2}\frac{\partial^2 u}{\partial y^2}+\frac{\nu}{R}\frac{\partial w}{\partial x})$$
$$S_y(u,v,w)=-K(\frac{\partial^2 v}{\partial y^2}+\frac{1-\nu}{2}\frac{\partial^2 v}{\partial x^2}+\frac{1+\nu}{2}\frac{\partial^2 u}{\partial x\partial y}+\frac{1}{R}\frac{\partial w}{\partial y})-$$
$$\frac{D}{R}(-\frac{\partial^3 w}{\partial y^3}+\frac{1}{R}\frac{\partial^2 v}{\partial y^2}+\frac{2(1-\nu)}{R}\frac{\partial^2 v}{\partial x^2}+(\nu-2)\frac{\partial^3 w}{\partial x^2\partial y}) \qquad (8)$$
$$S_z(u,v,w)=\frac{K}{R}(\nu\frac{\partial u}{\partial x}+\frac{\partial v}{\partial y}+\frac{w}{R})+D(\nabla^4 w-\frac{1}{R}\frac{\partial^3 v}{\partial y^3}+\frac{-(\nu-2)}{R}\frac{\partial^3 v}{\partial x^2\partial y})$$

in which, $\nabla^4 w=\frac{\partial^4 w}{\partial x^4}+2\frac{\partial^4 w}{\partial x^2\partial y^2}+\frac{\partial^4 w}{\partial y^4}$, and ρ= density of the shell material. For deriving the exact solutions for natural vibration modes from the differential equation of motion a spatial displacement pattern is taken in the form of double trigonometric series

$$u(x,y,t)=\sum_i\sum_j \overline{u}_{ij}cos\frac{j\pi x}{L}sin\frac{i\pi y}{R\phi}q_{ij}(t)$$
$$v(x,y,t)=\sum_i\sum_j \overline{v}_{ij}sin\frac{j\pi x}{L}cos\frac{i\pi y}{R\phi}q_{ij}(t)$$
$$w(x,y,t)=\sum_i\sum_j \overline{w}_{ij}sin\frac{j\pi x}{L}sin\frac{i\pi y}{R\phi}q_{ij}(t) \quad (9)$$

each mode of which satisfies the condition of simple supports.

$$v=w=0,\quad N_x=M_x=0\quad at\quad x=0,\ L$$
$$u=w=0,\quad N_\theta=M_\theta=0\quad at\quad y=0,\ R\,\phi \quad (10)$$

In the modal forms of Eq. (9), (i,j) represent the number of half waves in the circumferential and longitudinal directions respectively, and $\overline{u}_{ij}$, $\overline{v}_{ij}$, and $\overline{w}_{ij}$ are the normalized coefficient determined by solving the eigenvalue problem.

The generalized time response, used for solving the eigenvalue problem, is taken as $q_{ij}(t)=e^{m\omega_{ij}t}$ where $m^2=-1$, ω_{ij} is the natural radial frequency corresponding with the mode(i,j). Use of Eq. (9) allows Eq. (7) to be represented as an eigenvalue problem, in which the eigenvalues are associated with the natural frequencies, ω_{ij}, and the eigenmodes with amplitudes $\overline{u}_{ij}$, $\overline{v}_{ij}$, and $\overline{w}_{ij}$

$$\begin{bmatrix} a_{11} & a_{12} & a_{13}\\ a_{21} & a_{22} & a_{23}\\ a_{31} & a_{32} & a_{33}\end{bmatrix}\cdot\begin{Bmatrix} u_{ij}\\ v_{ij}\\ w_{ij}\end{Bmatrix}=\begin{Bmatrix}0\\0\\0\end{Bmatrix} \quad (11)$$

where

$$a_{11}=\lambda^2+\frac{(1-\nu)}{2}\frac{i^2\pi^2}{\phi^2}-\Delta_{ij}$$
$$a_{12}=a_{21}=\frac{\nu+1}{2}\lambda i\frac{\pi}{\phi}$$
$$a_{13}=-a_{31}=\nu\lambda$$
$$a_{22}=\frac{1-\nu}{2}\lambda^2+(\frac{i\pi}{\phi})^2\beta\left\{2(1-\nu)\lambda^2+(\frac{i\pi}{\phi})^2\right\}-\Delta_{ij}$$
$$a_{23}=a_{32}=-i\frac{\pi}{\phi}-\beta\left\{(2-\nu)\lambda^2\frac{i\pi}{\phi}+(\frac{i\pi}{\phi})^3\right\}$$
$$a_{33}=1+\beta\left(\lambda^2+(\frac{i\pi}{\phi})^2\right)^2-\Delta_{ij} \quad (12)$$

In these expressions $\lambda=\frac{\pi jR}{L}$, $\beta=\frac{h^2}{12R^2}$, and

$\Delta_{ij}=\frac{\rho(1-\nu^2)R^2}{Eg}(\omega_{ij})^2$ is a non-dimensionalized form of frequency. The resulting eigenvalue problem has been solved to extract frequencies for varying (i,j) with modal normalization based upon

$$\sqrt{(\overline{u}_{ij})^2+(\overline{v}_{ij})^2+(\overline{w}_{ij})^2}=1 \quad (1)$$

Once the mode shapes and natural frequencies of the open cylindrical shell have been obtained, the dynamic response of the structure can be computed from the mode superposition analysis.

2.2 Confirmation of Earthquake Dynamic Response

Once the mode shapes and natural frequencies of the open cylindrical shell have been obtained, the dynamic response of the structure can be computed from the mode superposition analysis. The dynamic equation of motion in the x, y, and z directions may be written in the form

$$F_x(u,v,w) = S_x(u,v,w) + c.\frac{\partial u}{\partial t} + \rho.h.\frac{\partial^2 u}{\partial t^2} - P_x(t) = 0$$
$$F_y(u,v,w) = S_y(u,v,w) + c.\frac{\partial v}{\partial t} + \rho.h.\frac{\partial^2 v}{\partial t^2} - P_y(t) = 0$$
$$F_z(u,v,w) = S_z(u,v,w) + c.\frac{\partial w}{\partial t} + \rho.h.\frac{\partial^2 w}{\partial t^2} - P_z(t) = 0 \qquad (2)$$

where c is the damping. In the present study the earthquake loading is considered to be an external force, which is modeled in terms of modal forces using a Fourier series representation of equivalent body forces ($P_x(t)$, $P_y(t)$, $P_z(t)$). The derivation of the equations governing the vibrations of open cylindrical shells follows the method used by Yamada [13]. To obtain the corresponding equations of motion in modal form the following procedure is considered. If Eq. (14) are satisfied then any weighted combination

$$\int_0^L \int_0^{R\phi} (F_x(u,v,w,t).u(x,y,t) + F_y(u,v,w,t).v(x,y,t)$$
$$+F_z(u,v,w,t).w(x,y,t))\,dx\,dy = 0 \qquad (3)$$

must also be satisfied. Substitution of Eq. (9), and (14) into Eq. (15) and taking the orthogonal properties of normal modes into account allows Eq. (15) to be rewritten as

$$\int_0^L \int_0^{R\phi} (S_x(u,v,w)u_{ij}q_{ij}(t) + c.\frac{\partial q_{ij}(t)}{\partial t}u_{ij}^2 + \rho.h.\frac{\partial^2 q_{ij}(t)}{\partial t^2}u_{ij}^2 - P_x(t)u_{ij}$$
$$+S_y(u,v,w)v_{ij}q_{ij}(t) + c.\frac{\partial q_{ij}(t)}{\partial t}v_{ij}^2 + \rho.h.\frac{\partial^2 q_{ij}(t)}{\partial t^2}u_{ij}^2 - P_y(t)v_{ij}$$
$$+ S_z(u,v,w)w_{ij}q_{ij}(t) + c.\frac{\partial q_{ij}(t)}{\partial t}w_{ij}^2 + \rho.h.\frac{\partial^2 q_{ij}(t)}{\partial t^2}w_{ij}^2 - P_z(t)w_{ij})dx\,dy = 0$$

(4)

For undamped free vibration $c = 0$ and $P_x(t) = P_y(t) = P_z(t) = 0$ allowing Eq. (16) to be written

$$\int_0^L \int_0^{R\phi} (S_x(u,v,w)u_{ij} + S_y(u,v,w)v_{ij} + S_z(u,v,w)w_{ij})dx\,dy = M_{ij}\omega_{ij}^2 \qquad (5)$$

in which the modal mass is represented as

$$M_{ij} = \rho.h\int_0^L \int_0^{R\phi} (u_{ij}^2 + v_{ij}^2 + w_{ij}^2)dx\,dy \qquad (18)$$

Using the modal normalization introduced in Eq. (13) a uniform distribution of mass in the open cylindrical shell results in a generalized modal mass that is constant in all modes, and given by

$$M_{ij} = \rho.h\frac{LR\phi}{4} \qquad (19)$$

Substitution of Eq. (17) and (18) into Eq. (16) results in

$$\omega_{ij}^2 M_{ij}q_{ij} + \frac{c}{\rho h}M_{ij}\frac{\partial q_{ij}}{\partial t} + M_{ij}\frac{\partial^2 q_{ij}}{\partial t^2}$$
$$= \int_0^L \int_0^{R\phi} (P_x(t)u_{ij} + P_y(t)v_{ij} + P_z(t)w_{ij})dx\,dy \qquad (6)$$

allowing the modal amplitudes of the shell's response to be determined from

$$\frac{\partial^2 q_{ij}}{\partial t^2} + 2\zeta_{ij}\omega_{ij}\frac{\partial q_{ij}}{\partial t} + \omega_{ij}^2 q_{ij} = \frac{P_{ij}}{M_{ij}} \tag{21}$$

where, $\zeta_{ij} = \frac{c}{2\omega_{ij}\rho h}$, is the modal damping ratio,

$$P_{ij}(t) = \int_0^L \int_0^{R\phi} (P_x(t)u_{ij} + P_y(t)v_{ij} + P_z(t)w_{ij})dx\,dy \tag{22}$$

In the absence of precise empirical information on modal damping, the modal damping ratio is considered constant in all modes, where implies c varies proportional to ω_{ij}.

Eq. (21) represents a set of uncoupled equations, which can be solved individually for each of the (i, j) modes using an analytical method. Once the modal responses $q_{ij}(t)$ have been determined they can be substitute in Eq. (9) to find the displacement time history responses for different locations on the roof shell. Shell stresses and strains are determined from Eq. (2), (3) and the acceleration time history responses are obtained from

$$\ddot{u}(x,y,t) = \sum_i \sum_j u_{ij}\ddot{q}_{ij}(t);\;\; \ddot{v}(x,y,t) = \sum_i \sum_j v_{ij}\ddot{q}_{ij}(t);\;\; \ddot{w}(x,y,t) = \sum_i \sum_j w_{ij}\ddot{q}_{ij}(t)$$

(7)

2.3 Modal Force

In the modal analysis the external forces need to be represented in terms of their modal components. If it is assumed that the loading is symmetric about the lines aa and bb of Fig.1 then only the odd modes will contribute to the total response of the shell. In this case the actual load P_z, P_y are represented spatially by two-dimensional Fourier series.

$$P_z \approx \sum_{i=1,3,5,\ldots} \sum_{j=1,3,5,\ldots} P_{z_{ij}} \sin\frac{j\pi x}{L} \sin\frac{i\pi y}{R\phi}$$
$$P_y \approx \sum_{i=1,3,5,\ldots} \sum_{j=1,3,5,\ldots} P_{y_{ij}} \sin\frac{j\pi x}{L} \cos\frac{i\pi y}{R\phi} \tag{24}$$

for which the Fourier coefficient are given by

$$P_{zij} = \frac{\int_0^L \int_0^{R\phi} P_z \sin\frac{j\pi x}{L} \sin\frac{i\pi y}{R\phi} dx\,dy}{\int_0^L \int_0^{R\phi} \sin^2\frac{j\pi x}{L} \sin^2\frac{i\pi y}{R\phi} dx\,dy}$$
$$P_{y_{ij}} = \frac{\int_0^L \int_0^{R\phi} P_y \sin\frac{j\pi x}{L} \cos\frac{i\pi y}{R\phi} dx\,dy}{\int_0^L \int_0^{R\phi} \sin^2\frac{j\pi x}{L} \cos^2\frac{i\pi y}{R\phi} dx\,dy} \tag{25}$$

When the shell supports are subjected to a synchronized vertical acceleration $a_{gv}(t)$, the time dependent body forces are

$$P_z = \overline{P}cos(-\frac{\phi}{2} + \frac{y}{R})$$
$$P_y = \overline{P}sin(-\frac{\phi}{2} + \frac{y}{R}) \tag{26}$$

where $\overline{P} = \rho h a_{gv}(t)$, which upon substitution of Eq. (9) and (25) into Eq. (22), permits the modal force to be represented as

$$P_{ij}(t) = \rho h L R \phi a_{gv}(t) \frac{(-1+cos i\pi)(-1+cos j\pi)(\overline{w} i\pi - \overline{v}\phi)}{j\pi(i\pi-\phi)(i\pi+\phi)} cos\frac{\phi}{2} \quad (8)$$

The horizontal earthquake acting normal to the axis of the shell, is derived using the procedure similar to that outlined for the vertical component of the earthquake, except that just the even harmonics i are involved. For the horizontal earthquake component modal force can be represented as

$$P_{ij}(t) = \rho h L R \phi a_{gh}(t) \frac{(1+cos i\pi)(-1+cos j\pi)(-\overline{w} i\pi - \overline{v}\phi)}{j\pi(-i\pi+\phi)(i\pi+\phi)} sin\frac{\phi}{2} \quad (9)$$

For a particular earthquake record $a_{gv}(t)$, $a_{gh}(t)$ the modal loads of Eq (27), (28) allow the modal displacement q_{ij} to be found from Eq (21).

2.4 Selected earthquake ground motion

Landers earthquake measured on June 28th 1992 at the Lucrene station with duration of $48.12\ s$ is used for this study. The vertical component of Landers earthquake has a Peak Ground Acceleration (PGA) of $0.818\ g$ as shown in Fig.2(a) with a $0.005\ s$ time interval of recorded data. The frequency content of vertical component shown in Fig.2(b) indicates that most of the energy in the accelerogram is in the frequency range up to $45\ Hz$ and the largest amplitude is at a frequency approximately $14\ Hz$. The reason for choosing this earthquake is because the earthquake has significant energy over a wide range of frequencies and especially around high frequencies. As the natural frequencies of cylindrical shell also have a wide range and includes modes with high frequency, the choice of this earthquake should help to investigate the possible contribution of the modes with high frequencies in the response. The displacement and acceleration response spectra are then derived and reported in Fig. 2(c),(d) for a 5% damped system subjected to the vertical component of Landers earthquake.

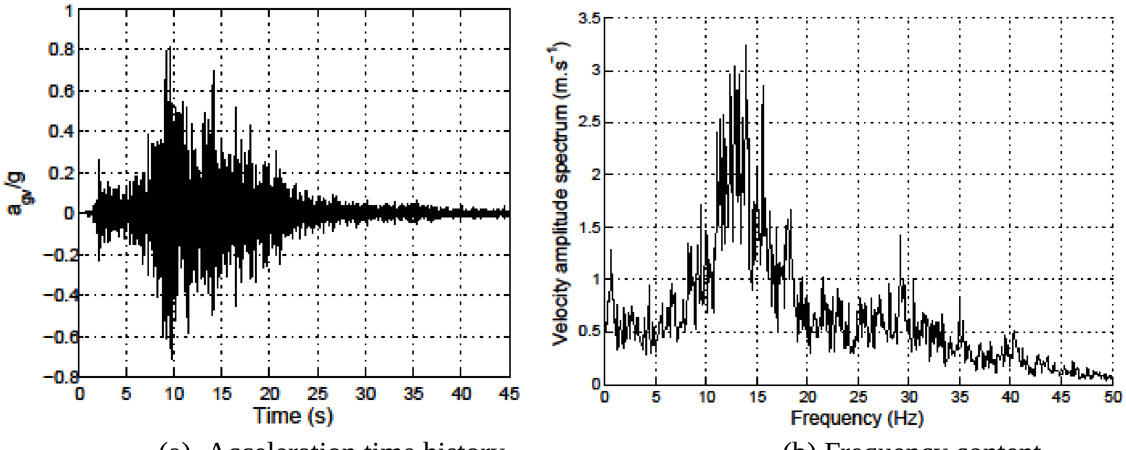

(a) Acceleration time history (b) Frequency content

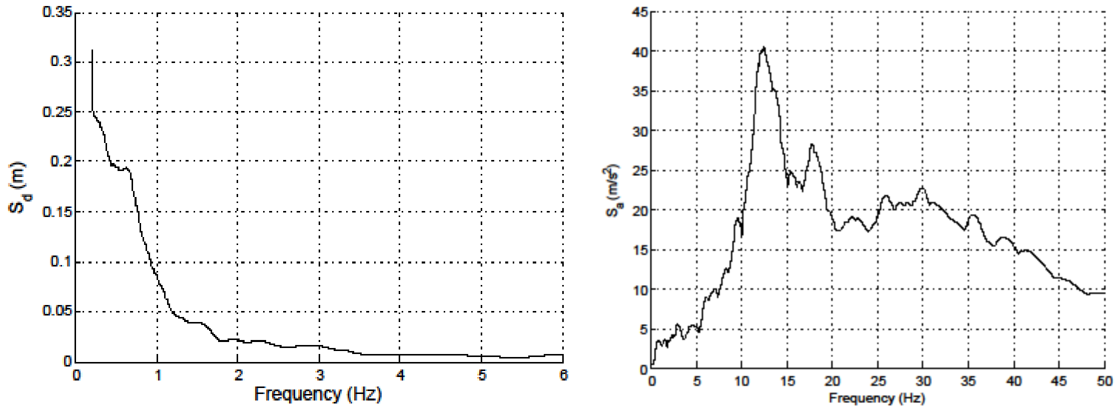

(c) Displacement response spectrum for 5% damped system

(d) Acceleration response spectrum for 5% damped system

Fig. **2 –** Vertical component of Landers earthquake

The displacement and acceleration response spectrum is also derived and presented in Fig.2(c),(d) for a 5% damped system. The horizontal component has a $PGA = 0.789\ g$ and again the earthquake data is available for every $0.005\ s$.

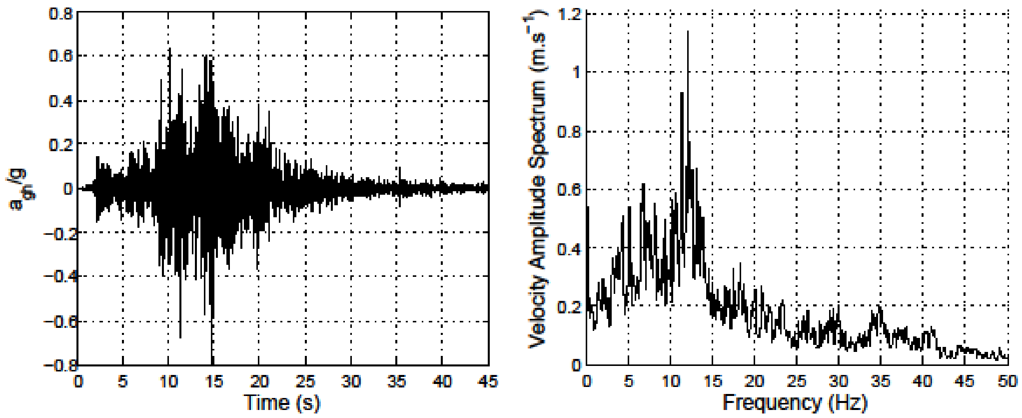

(a) Acceleration time history

(b) Frequency content

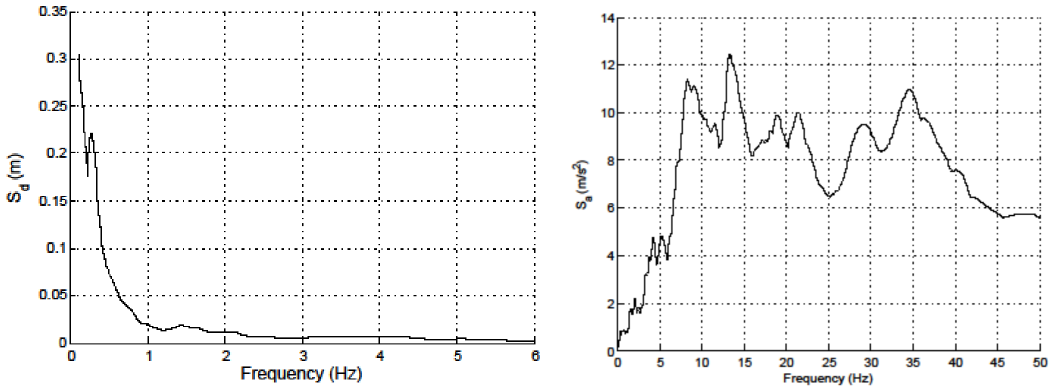

(c) Displacement response spectrum for 5% damped system

(d) Acceleration response spectrum for 5% damped system

Fig. **3 –** Horizontal component of Landers earthquake

As can be seen, the Landers earthquake has a high ratio of vertical to horizontal peak ground acceleration, which makes it a suitable choice to show the conditions that the vertical component of an earthquake can result in higher responses than the horizontal components of an earthquake. However, it should be noted that this earthquake is not a typical earthquake and such records can only happen in near-field events.

2.5 Response of structures to vertical and horizontal components of earthquake

The seismic analysis of structures is usually performed for horizontal component of earthquakes with the vertical component often neglected. In this paper the response of shells under vertical components of earthquake is investigated. However, as explained earlier in order to highlight the conditions that the vertical component of earthquake could result in higher responses, Landers earthquake with a high vertical component compared to its horizontal component is chosen. It should be noted that the earthquakes with high vertical to horizontal components usually occur in near-field events. In order to find the relative importance of vertical and horizontal components of earthquakes the maximum acceleration and stress resultants were found for a range of shells with $R/h = 500$, $\phi = \pi/3$, $B = \rho\, R\, h/E$ between 0.5 to $2 \times 10^{-6}\ s^2$, and $L_y/L_x = 0.5,\ 1,\ 2$. The results are presented in Fig.4. The shells are subjected to the horizontal and vertical component of Landers earthquake as in Fig.2 and 3.

For simplicity of comparison, the maximum responses to vertical and horizontal component of earthquake (Fig.2, 3) are shown in Fig.4, in which the solid lines represent the responses of shells to vertical components of the Landers earthquake, while the dashed lines show the responses of shells to horizontal components of the same earthquake.

Looking at Fig.4, it is clear that the vertical components of the this earthquake lead to significantly higher displacements, accelerations, and stresses compared with the horizontal component of it. This can be explained by comparing the acceleration response spectrum in Fig.2(d), and 3(d), showing that at each specific frequency the acceleration response spectrum of vertical component of Landers earthquake is considerably higher than the horizontal component. So the response of each individual mode of the shell having these frequencies to the vertical component of the Landers earthquake is higher than the horizontal component of this earthquake. For example, for a mode having $f = 10\ Hz$, the acceleration response spectrum of the horizontal component of earthquake is $S_a = 10\ m/s^2$ (Fig.3(d)), which is less than the acceleration response spectrum of vertical component of earthquake equal to $S_a = 18\ m/s^2$ (Fig.2(d)). This study involves considering a total number of 19 half-waves in circumferential and axial directions, the results indicates that the sum of the responses of these modes to the vertical component of Landers earthquake would be higher than the responses when subjected to horizontal component of the Landers earthquake as shown in Fig.4.

Fig.4(c)-(e) show the stress resultants are also higher when shells are subjected to the vertical component of the selected earthquake. It is because the stress resultants are dependent to displacement response spectrum. Displacement response spectrum is shown to have higher responses to vertical component of Landers earthquake (Fig.2(c), Fig.3(c)).

To better understand this, a shell with $B = 1 \times 10^{-6}\ s^2$ and $L_y/L_x = 1$ is chosen; Fig.4(c) shows the axial membrane stress resultant is higher when the shell is subjected to vertical component of the Landers earthquake. According to Fig.5(d), the most contributing modes in axial membrane stress resultant for this shell are $(i, j) = (1, 1)$, $(3, 1)$, $(5, 1)$, and $(5, 3)$ with the corresponding frequencies as $f_{1,1} = 3.589\ Hz$, $f_{3,1} = 0.8586\ Hz$, $f_{5,1} = 1.0483\ Hz$, $f_{5,3} = 2.5\ Hz$. Using Fig.2(c) and 3(c), the displacement response spectrum corresponding to mode $(1, 1)$, $(3, 1)$, $(5, 1)$, and $(5, 3)$ are equal to $0.015\ m$, $0.025\ m$, $0.07\ m$, and $0.12\ m$, respectively when subjected to vertical component of earthquake (Fig.2). They reduce to $0.015\ m$, $0.015\ m$, $0.02\ m$, and $0.04\ m$, respectively when subjected to horizontal component of earthquake. This explains the reason for the reduction in N_x when the shell is subjected to horizontal component of the earthquake.

Fig.4 highlights the importance of considering the vertical component of earthquakes, in the design of this form of shell.

As can be seen from Fig.4, the responses to earthquake components are significantly dependent on the shell geometry and material properties so that this conclusion may need to be reassessed for shells with different geometric and material parameters.

Responses can however vary for shell with various material properties. This is a result of the shells having different range of natural frequencies, which depending on the displacement response spectrum of the earthquake can result in different responses.

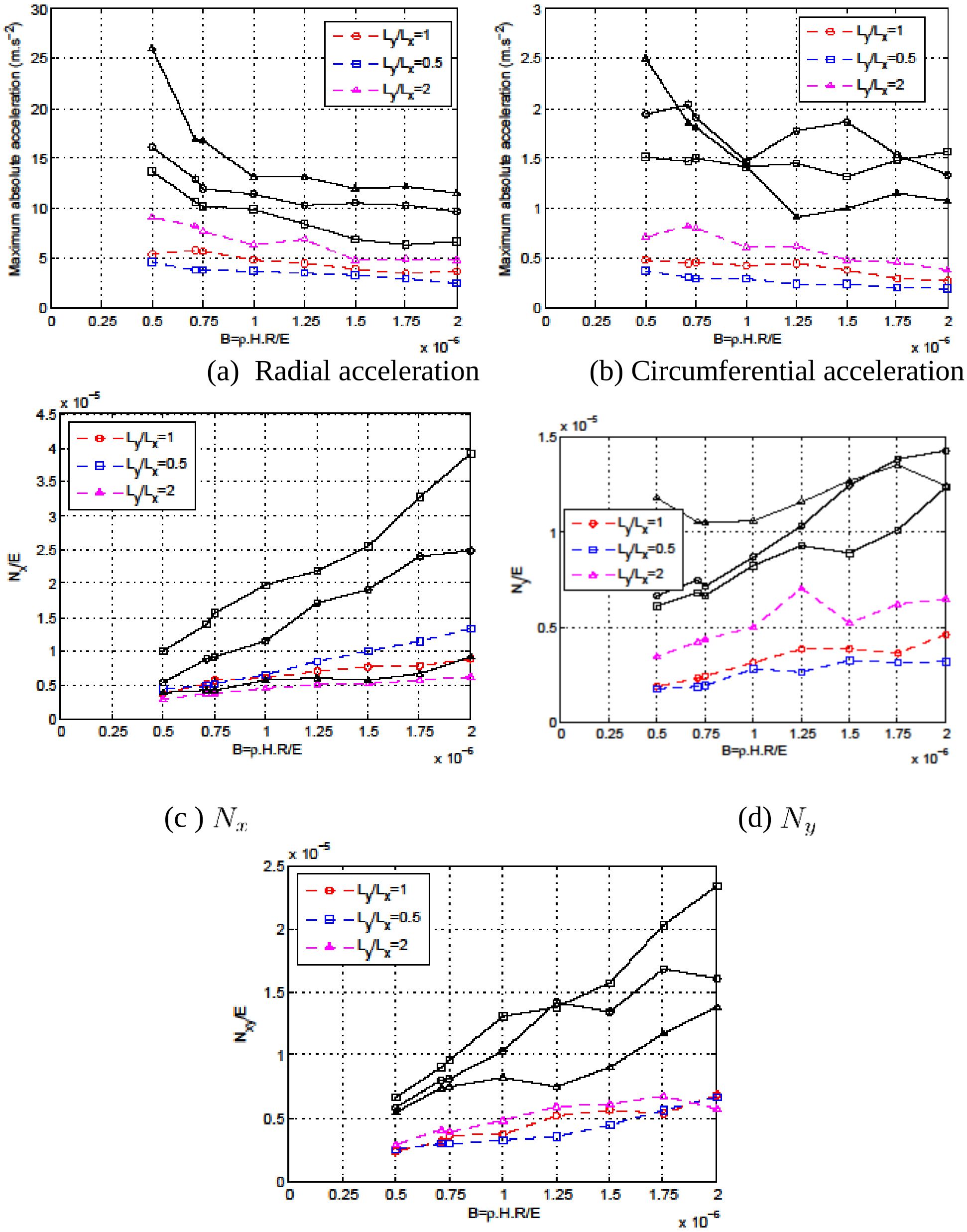

(a) Radial acceleration (b) Circumferential acceleration

(c) N_x (d) N_y

(e) N_{xy}

Fig. **4 –** Comparison of maximum absolute acceleration and stress for horizontal and vertical components of Landers earthquake, $R/h = 500$, $\phi = \pi/3$. Solid lines represent the responses of shells to the vertical component of the Landers earthquake. Dashed lines represent the responses of shells to horizontal component of the Landers earthquake.

3. Conclusions

Using an analytical method, the relative importance of vertical and horizontal component of a selected earthquake on cylindrical roof shells has been investigated. Many studies are performed for the horizontal component of an earthquake, while the vertical component is usually neglected. However, this investigation has demonstrated that the displacements, accelerations, and stress resultants have been increased when shells are subjected to the vertical component of an earthquake than those of the horizontal components. It should be noted that as the objective of this research is to highlight the conditions that vertical component of earthquakes could produce higher responses compared to the horizontal component of earthquake, Landers earthquake has been chosen. This earthquake has a high ratio of vertical to horizontal ground peak acceleration. It is also worth noting that the relative importance of the horizontal and vertical components of earthquake depends on the relationship between the frequency spectrum of the selected earthquake and natural frequencies of the shell. This study suggests that in order to obtain sufficiently reliable prediction of the earthquake response of cylindrical shell roofs, and by inference other forms of shell, it is important to include the vertical component of the earthquake in the analysis.

4. References

[1] Broderick BM, Elnashai AS (1995): Analysis of the failure of interstate 10 freeway ramp during the northridge earthquake of 17 January 1994. *Earthquake Engineering & Structural Dynamics*, **24**(2), 189–209.

[2] Papazoglou AJ, Elnashai AS (1996): Analytical and field evidence of the damaging effect of vertical earthquake ground motion. *Earthquake Engineering & Structural Dynamics*, **25**(10), 1109–1138.

[3] Kunnath SK, Erduran E, Chai YH, Yashinsky M (2008): Effect of near-fault vertical ground motions on seismic response of highway overcrossings. *Journal of Bridge Engineering*, **13**(3), 282-290.

[4] Bozorgnia Y, Niazi M (1993): Distance scaling of vertical and horizontal response spectra of the Loma Prieta earthquake. *Earthquake engineering & Structural Dynamics*, **22**(8), 695–707.

[5] Bozorgnia Y, Campbell KW (2004): The vertical-to-horizontal response spectral ratio and tentative procedures for developing simplified v/h and vertical design spectra, *Journal of Earthquake Engineering*, **8**(2), 175–207.

[6] Ambraseys NN, Simpson KA (1996): Prediction of vertical response spectra in Europe. *Earthquake Engineering & Structural Dynamics*, **25**(4), 401–412.

[7] Elgamal A, He L (2004): Vertical earthquake ground motion records: An overview. *Journal of Earthquake Engineering*, **8**(5), 663–697.

[8] Collier CJ, Elnashai AS (2001): A procedure for combining vertical and horizontal seismic action effects. *Journal of Earthquake Engineering*, **5**(4), 521–539.

[9] Elnashai AS , Papazoglou AJ (1997): Procedure and spectra for analysis of RC structures subjected to strong vertical earthquake loads. *Journal of Earthquake Engineering*, **1**(1), 121–155.

[10] Kim SJ, Holub CJ, Elnashai AS (2010): Analytical assessment of the effect of vertical earthquake motion on RC bridge piers. *Journal of Structural Engineering*, **137**(2), 252-260.

[11] Leissa AW (1973): Vibration of shells. NASA.

[12] Qatu MS (2002): Recent research advances in the dynamic behavior of shells: 1989-2000, Part 1: Laminated composite shells. *Applied Mechanics Reviews*. **55**(4), 325-350.

[13] Yamada S (1997): Vibration behaviour of single-layer latticed cylindrical roofs. *International Journal of Space Structures*, **12**(3-4), 181-190.

[14] Kunieda H (1997): Earthquake response of roof shells. *International Journal of Space Structures,* 12(3), 149-169.